Masterarbeit

Waqar Ahmed

Deep Learning of Cardiac Related Condition using a Non-Contact Multi-Sensor System

LEHRSTUHL FÜR MEDIZINISCHE INFORMATIONSTECHNIK
Fakultät für Elektrotechnik und Informationstechnik, RWTH Aachen
Univ.-Prof. Dr.-Ing. Dr. med. Steffen Leonhardt
Betreuer-/in: Dipl.-Ing. Anake Pomprapa
Datum: 25. Dezember 2017

Acknowledgments

Lorem ipsum dolor sit amet, consetetur sadipscing elitr, sed diam nonumy eirmod tempor invidunt ut labore et dolore magna aliquyam erat, sed diam voluptua. At vero eos et accusam et justo duo dolores et ea rebum. Stet clita kasd gubergren, no sea takimata sanctus est Lorem ipsum dolor sit amet. Lorem ipsum dolor sit amet, consetetur sadipscing elitr, sed diam nonumy eirmod tempor invidunt ut labore et dolore magna aliquyam erat, sed diam voluptua. At vero eos et accusam et justo duo dolores et ea rebum. Stet clita kasd gubergren, no sea takimata sanctus est Lorem ipsum dolor sit amet. Lorem ipsum dolor sit amet, consetetur sadipscing elitr, sed diam nonumy eirmod tempor invidunt ut labore et dolore magna aliquyam erat, sed diam voluptua. At vero eos et accusam et justo duo dolores et ea rebum. Stet clita kasd gubergren, no sea takimata sanctus est Lorem ipsum dolor sit amet.

Duis autem vel eum iriure dolor in hendrerit in vulputate velit esse molestie consequat, vel illum dolore eu feugiat nulla facilisis at vero eros et accumsan et iusto odio dignissim qui blandit praesent luptatum zzril delenit augue duis dolore te feugait nulla facilisi. Lorem ipsum dolor sit amet, consectetuer adipiscing elit, sed diam nonummy nibh euismod tincidunt ut laoreet dolore magna aliquam erat volutpat.

Ut wisi enim ad minim veniam, quis nostrud exerci tation ullamcorper suscipit lobortis nisl ut aliquip ex ea commodo consequat. Duis autem vel eum iriure dolor in hendrerit in vulputate velit esse molestie consequat, vel illum dolore eu feugiat nulla facilisis at vero eros et accumsan et iusto odio dignissim qui blandit praesent luptatum zzril delenit augue duis dolore te feugait nulla facilisi.

Eidesstattliche Versicherung

Name, Vorname

Matrikelnummer (freiwillige Angabe)

Ich versichere hiermit an Eides Statt, dass ich die vorliegende Arbeit/Bachelorarbeit/ Masterarbeit* mit dem Titel

selbständig und ohne unzulässige fremde Hilfe erbracht habe. Ich habe keine anderen als die angegebenen Quellen und Hilfsmittel benutzt. Für den Fall, dass die Arbeit zusätzlich auf einem Datenträger eingereicht wird, erkläre ich, dass die schriftliche und die elektronische Form vollständig übereinstimmen. Die Arbeit hat in gleicher oder ähnlicher Form noch keiner Prüfungsbehörde vorgelegen.

Ort, Datum

Unterschrift

*Nichtzutreffendes bitte streichen

Belehrung:

§ 156 StGB: Falsche Versicherung an Eides Statt

Wer vor einer zur Abnahme einer Versicherung an Eides Statt zuständigen Behörde eine solche Versicherung falsch abgibt oder unter Berufung auf eine solche Versicherung falsch aussagt, wird mit Freiheitsstrafe bis zu drei Jahren oder mit Geldstrafe bestraft.

§ 161 StGB: Fahrlässiger Falscheid; fahrlässige falsche Versicherung an Eides Statt

(1) Wenn eine der in den §§ 154 bis 156 bezeichneten Handlungen aus Fahrlässigkeit begangen worden ist, so tritt Freiheitsstrafe bis zu einem Jahr oder Geldstrafe ein.

(2) Straflosigkeit tritt ein, wenn der Täter die falsche Angabe rechtzeitig berichtigt. Die Vorschriften des § 158 Abs. 2 und 3 gelten entsprechend.

Die vorstehende Belehrung habe ich zur Kenntnis genommen:

Ort, Datum

Unterschrift

Abstract

Lorem ipsum dolor sit amet, consetetur sadipscing elitr, sed diam nonumy eirmod tempor invidunt ut labore et dolore magna aliquyam erat, sed diam voluptua. At vero eos et accusam et justo duo dolores et ea rebum. Stet clita kasd gubergren, no sea takimata sanctus est Lorem ipsum dolor sit amet. Lorem ipsum dolor sit amet, consetetur sadipscing elitr, sed diam nonumy eirmod tempor invidunt ut labore et dolore magna aliquyam erat, sed diam voluptua. At vero eos et accusam et justo duo dolores et ea rebum. Stet clita kasd gubergren, no sea takimata sanctus est Lorem ipsum dolor sit amet. Lorem ipsum dolor sit amet, consetetur sadipscing elitr, sed diam nonumy eirmod tempor invidunt ut labore et dolore magna aliquyam erat, sed diam voluptua. At vero eos et accusam et justo duo dolores et ea rebum. Stet clita kasd gubergren, no sea takimata sanctus est Lorem ipsum dolor sit amet.

Duis autem vel eum iriure dolor in hendrerit in vulputate velit esse molestie consequat, vel illum dolore eu feugiat nulla facilisis at vero eros et accumsan et iusto odio dignissim qui blandit praesent luptatum zzril delenit augue duis dolore te feugait nulla facilisi. Lorem ipsum dolor sit amet, consectetuer adipiscing elit, sed diam nonummy nibh euismod tincidunt ut laoreet dolore magna aliquam erat volutpat.

Ut wisi enim ad minim veniam, quis nostrud exerci tation ullamcorper suscipit lobortis nisl ut aliquip ex ea commodo consequat. Duis autem vel eum iriure dolor in hendrerit in vulputate velit esse molestie consequat, vel illum dolore eu feugiat nulla facilisis at vero eros et accumsan et iusto odio dignissim qui blandit praesent luptatum zzril delenit augue duis dolore te feugait nulla facilisi.

Inhaltsverzeichnis

Symbols

1 Abbreviations

AV	atrioventricular
ECG	electrocardiogram
RT	re-polarization time
SA	sino-atrial

Abkürzungen

H_2O	Wasser
RWTH Aachen	Rheinisch-Westfälische Technische Hochschule Aachen
DPO	Diplomprüfungsordnung

Physikalische Größen

v	Geschwindigkeit	$\frac{km}{h}$
t	Zeit	h

Mathematische Größen

M	mathematische Beispielgröße

Indizes

k	Anzahl der Prozeßschritte
$P_1...P_n$	Prozeßschritt P_1 bis P_n
V_{Ziel}	Zielvektor

Konstanten

π	3.141592653589

1 Introduction

1.1 Anatomy of Heart

The function of the heart is to pump the blood inside the body, which is stimulated by an electrical stimulus. The heart pumps blood thorugh the arteries, veins to the different parts of the body such as organs, muscles and tissues.

The heart is made up of 4 chambers, left and right atria, and left and right ventricles,as can be seen in Figure 1.1. The right atrium receives de-oxygenated blood from the whole body and pumps it into the right ventricle which then pumps the blood to the lungs for oxygenation. The left atrium receives oxygenated blood from the lungs and pumps it into the left ventricles which then pumps the oxygenated blood to the whole body. The aorta carries oxygenated blood to the different part of the body and the pulmonary arteries carry the de-oxygenated blood back to the lungs for oxygenation. The important point to note here is that, the blood flows to different organs via arteries and returns back to heart via veins.

The main components of the cardiac conduction system are:

1. Synoatrial (SA) Node
2. The Atrioventricular (AV) Node
3. Atrioventricular (AV) Bundle or Bundle of His
4. Right and Left Bundle Branches
5. Purkinje Fibers

The SA node, also known as sinus node, is a natural pacemaker of the heart which is located at the right atrium. It produces an electric stimulus at the rate of 60 to 100 signals per minute (under normal condition), which travels through the heart to make it pump the blood to the body. It initiates all heart beats and determine the heart rate. Electrical impulse from the SA node spread throughout the atrium which results in the contraction of the atrium. The AV node which is located on the other side of right atrium, near the AV valve. The purpose of this node is to serve as a gateway to the ventricles. It also delays the passage of electrical impulse to the ventricles. It is to ensure that, all the blood is ejected from the atria to the ventricles before the ventricles contract. The AV node then passes the signal to the atrioventricular (AV) bundle or bundle of His. The bundle is divided into two parts, right and left bundle branches to stimulate the right and left ventricles. The signal is then travels down to the Purkinje fibers where from the signal spreads upwards

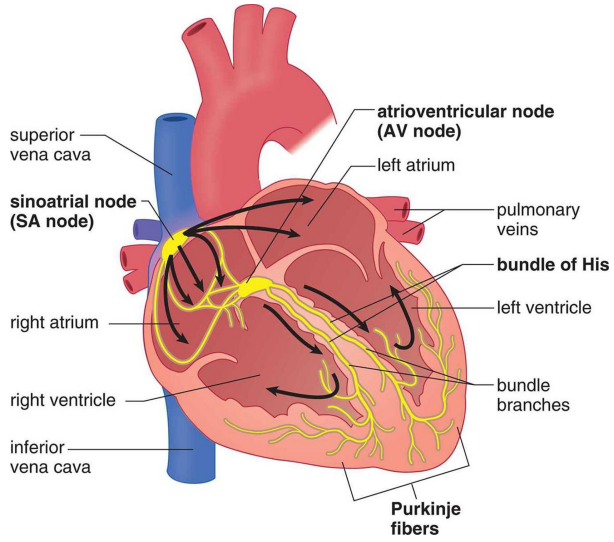

Figure. 1.1: The electrical activity of heart, taken from [Sch17].

throughout the ventricular myocardium. Each contraction of the ventricles represents one single heartbeat.

Each heartbeat is composed of two phases, known as systole and diastole. During **systole**, the heat muscles contract and the blood is pumped from ventricles to the different parts of the body. During **diastole**, the hearts muscles relax and the blood from atria flows into the ventricles. The pressure generated during systole from the ventricular contraction is high, whereas, during diastole, the muscle relaxation reduces this pressure.

The electrical activity of the heart can be detected in the form of Electrocardiogram by placing electrodes on the body surface. It is a powerful tool for diagnosing the status of patient's heart.

1.2 The Electrocardiogram

Electrocardiogram (ECG) is an essential tool for diagnosing the electrical activity of the heart. It is a simple, non-invasive procedure to measure the activity of the heart. Most of the tools available today to measure the ECG are based on the electrodes which are required to be attached to the body. The electrodes sense the electrical currents inside the body and transmit them to the ECG monitor. These currents are then transformed into appropriate waveforms which represent the heart's polarization and depolarization cycle. Different components of the wave represent activity of different parts of the heart.

In conventional 12-lead ECG, 10 electrodes or leads are attached to the patient's body and then the electrical activity of heart is viewed from 12 different perspectives. These

12 views of heart are captured by placing the electrodes on chest, wrists, and ankles. The main purpose of ECG is to identify any cardiac arrhythmia, ischemia, problems with heart rate or irregularities.

These 10 electrodes are divided into 2 groups.

1. 6 chest electrodes

2. 4 limb electrodes

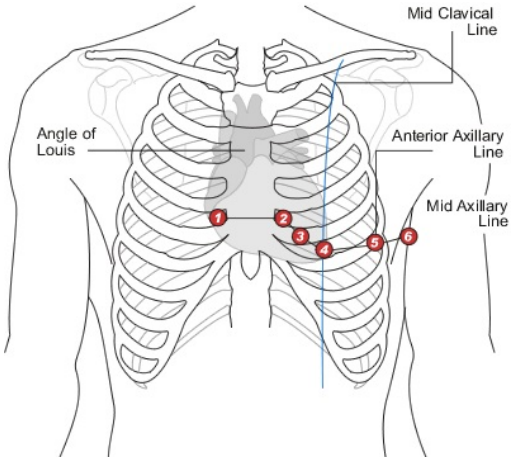

Figure. 1.2: The leads position on chest, taken from [The].

Chest Electrodes

The chest electrodes are denoted as "V" and they all are numbered from V1 to V6 as can be seen in Figure 1.2. The electrodes are positioned at the following locations on the chest:

- V1 - Fourth intercostal space (between ribs 4 and 5) on the right sternum
- V2 - Fourth intercostal space (between ribs 4 and 5) on the left sternum
- V3 - Placed in the middle of V2 and V4
- V4 - Fifth intercostal space (between ribs 5 and 6) at the mid-clavicular line
- V5 - Placed horizontally on anterior axillary line with V4
- V6 - Placed horizontally on Mid-axillary line with V4 and V5

The 3 different axillary lines **anterior axillary line**, **midaxillary line**, and **posterior axillary line** can be seen in Figure 1.3.

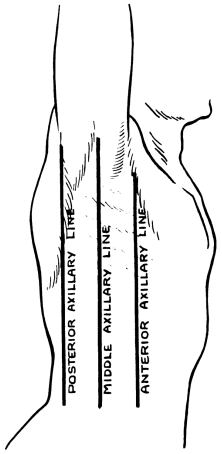

Figure. 1.3: The axillary lines on the right side of chest, taken from [Com17a].

Limb Electrodes

The 4 limb electrodes are denoted as RA, LA, LL, RL and there respective positions are:

- RA - Anywhere on right arm between shoulder and elbow, but avoiding thick muscles.
- LA - Symmetric to the RA position, but on left arm
- RL - Anywhere on right leg between the torso and the ankle
- LL - Symmetric to the RL position, but on left leg

The limb electrodes are shown in Figure 1.4

1.3 ECG Complex

ECG complex represents the electrical activity of heart during one cardiac cycle. A normal cardiac cycle consists of five waveforms labeled with P, Q, R, S and T as can be seen in Figure 1.5. The Q, R and S waves are referred to as one unit, the QRS complex. The ECG signal represents the conduction of electrical impulses from the atria to the ventricles. The important parameters in the ECG signal are:

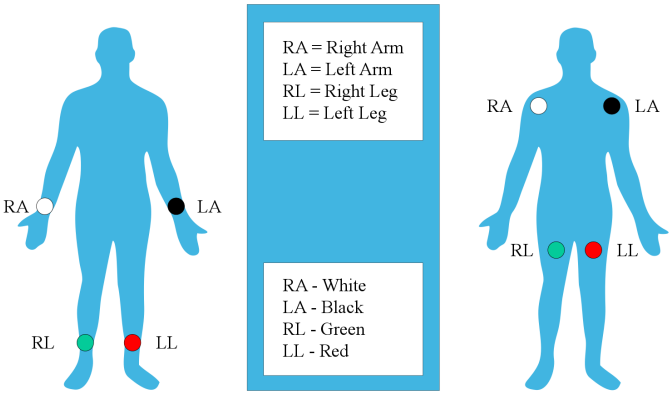

Figure. 1.4: The possible position of limb leads, taken from [Com17b].

1.3.1 P Wave

The P wave is the first component of the ECG signal. It occurs due to contraction of the both left and right atrium. This process also known as atrial depolarization. A normal P wave has following characteristics (in lead II):

- duration: 0.06 to 0.12 seconds
- amplitude: 2 to 3 mm high
- location: before the QRS complex

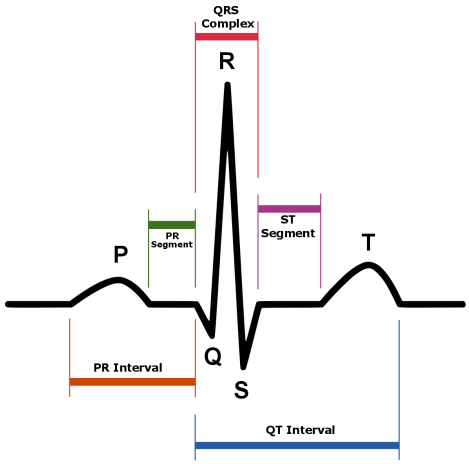

Figure. 1.5: The ECG signal, taken from [Com17c].

1.3.2 QRS Complex

The QRS complex follows the P wave and represents contraction of the both right and left ventricles. This contraction results in the blood ejection from the heart which eventually pumps into the arteries, creating a pulse. The Q and S waves are relatively very small whereas, R wave is comparatively very big. A normal QRS complex has following characteristics (in lead II):

- duration: 0.06 to 0.10 seconds
- amplitude: 5 to 30 mm high
- location: follows the P wave

1.3.3 T Wave

The T wave represents the ventricle re-polarization. It occurs during the last part of ventricle systole. The T wave has following characteristics (in lead II):

- duration: 0.10 to 0.25 seconds or greater
- amplitude: <5 mm high
- location: follows the QRS complex

1.3.4 PR Interval

The PR interval is the time interval between the end of contraction of the atrium and beginning the contraction of the ventricles. A normal PR interval has following characteristics:

- duration: 0.12 to 0.20 seconds
- location: From the beginning of P wave to the beginning of the QRS complex

1.3.5 ST Segment

The ST segment represents the end of ventricular depolarization and the beginning of the ventricles relaxation. The Point between the end of QRS complex and the beginning of ST segment is called as the J point. A normal ST segment has following characteristics:

- duration: 0.08 to 0.12 seconds
- location: From the end of QRS complex to the beginning of T wave

1.3.6 QT Interval

The QT interval is the time interval between the ventricular depolarization and repolarization. The QT duration varies according to the heart rate. Faster heart rate results in smaller QT interval whereas, slower heart rate may results in bigger QT interval. The bigger QT interval may results in irregular heart beat. A normal QT interval has following characteristics:

- duration: 0.36 to 0.44 seconds
- location: From the beginning of QRS complex to the end of T wave

1.4 Disadvantages of Attached Electrodes

While it is easy to monitor the electrical heart activity by placing the electrodes directly on the body but it has several disadvantages as well.

- It limits the patient's mobility.
- Discomfort for the patient as electrodes are directly attached to the body.
- Loss of cardiac monitoring in case if patient moves.
- Long contact of the electrodes may irritate the skin.

1.5 Noise in ECG Signal

Most of the time, the ECG signal is corrupted by the different types of noises and artifacts which changes the characteristics of the ECG signal [LD]. Hence, it becomes very difficult to extract the useful information from the signal. Following are the major noises which are present in the ECG signal.

1.5.1 Power Line Interference

Power line interference is a 60 Hz noise which is present in ECG signal because of improper grounding of the ECG equipment or interference from the nearby equipment. In order to remove this type of noise, a proper use of filter is required. A 60 Hz notch filter can be used to remove the power line interference. Figure 1.6 illustrates the 60 Hz power line interference in ECG signal.

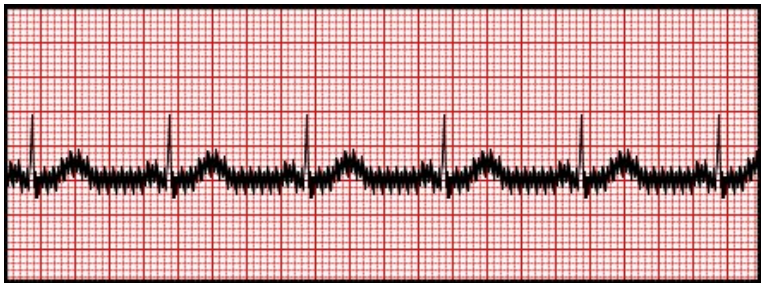

Figure. 1.6: 60 Hz AC Interference, taken from [mau17].

1.5.2 Baseline wander

Baseline wander is a low frequency components which corrupt the ECG signal because of breathing, body movements, dirty or loose electrodes , electrode impedance, etc. Generally they have frequency greater than 1 Hz. A high pass filter can be used to remove the baseline wander. The baseline wandering in ECG signal can be seen in Figure 1.7.

1.5.3 Muscle Noise

This type of noise is caused by muscle contractions besides heart which results in the change of heart electric potential [MG13]. When the other muscles near the electrodes depolarized and re-polarized, they also generate waves which is then picked up by the ECG. They generally occur in short time burst and have higher amplitude values than the

Figure. 1.7: Baseline wandering in ECG signal, taken from [mau17].

ECG signal. It can be removed using wavelet transform [MPS+11]. An example of ECG signal effected by muscle contractions can be seen in figure 1.8.

Figure. 1.8: ECG signal combined with muscle noise , taken from [mau17].

1.6 Arrhythmias

Irregularity in the heartbeat is known as arrhythmia (also called dysrhythmia) [med17]. During arrhythmia, a heart is out of normal rhythm and may feel like the heart is skipped a beat or beat with an irregular pattern. A normal heart rate lies between 60 to 100 beats per miutes and arrhythmia can occur with normal heart rate, slow heart rate (called bradycardia) in which heart rate is less than 60 beats per minute or with rapid heart rate (called tachycardia) in which heart beats faster than 100 beats per minute.

1.6.1 Causes of an Arrhythmia

Arrhytmia can be caused by one of the following reasons:

- Heart disease
- Electrolyte imbalance

- Changes in heart muscle
- After surgery effects

1.6.2 Types of Arrhythmias

The most common types of arrhythmias are:

Premature Ventricular Contraction

It is a type of arrhythmia in which the heart beat is initiated by the ventricles rather than the SA node. It is is generally refers as ßkipped beats". This is the most common type of arrhythmia which occurs with or without any heart disease. It could be the result of too much stress, usage of too much cocaine or restless. But sometimes it can also be caused by heart disease. Most of the time PVC are considered as harmless and rarely need a treatment.

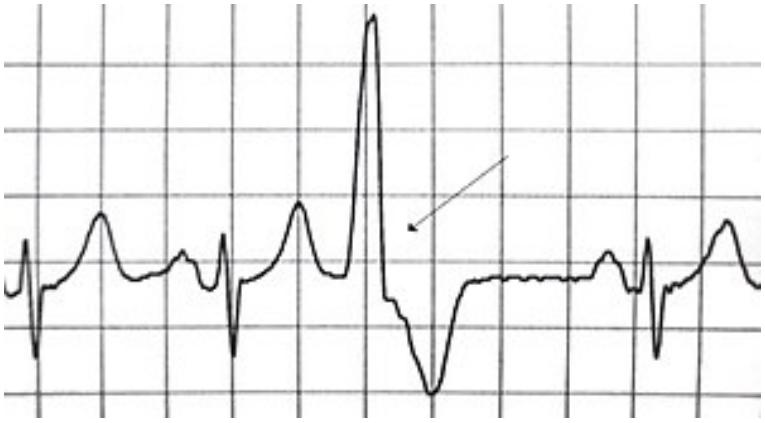

Figure. 1.9: Premature Ventricular Contraction, taken from [con17].

Atrial Fibrillation

This type of arrhythmia caused by the abnormal contraction of the upper chamber of heart. During atrial fibrillation, the atria beats irregularly without any coordination with the ventricles. This could results in heart palpation, shortness of breath and weakness.

Atrial Flutter

This type of arrhythmia caused by problems in the heart's electrical system. It is similar to atrial fibrillation but rhythm in atria is more organized than the atrial fibrillation. The risk factors and causes of atrial flutter are similar to those of atrial fibrillation.

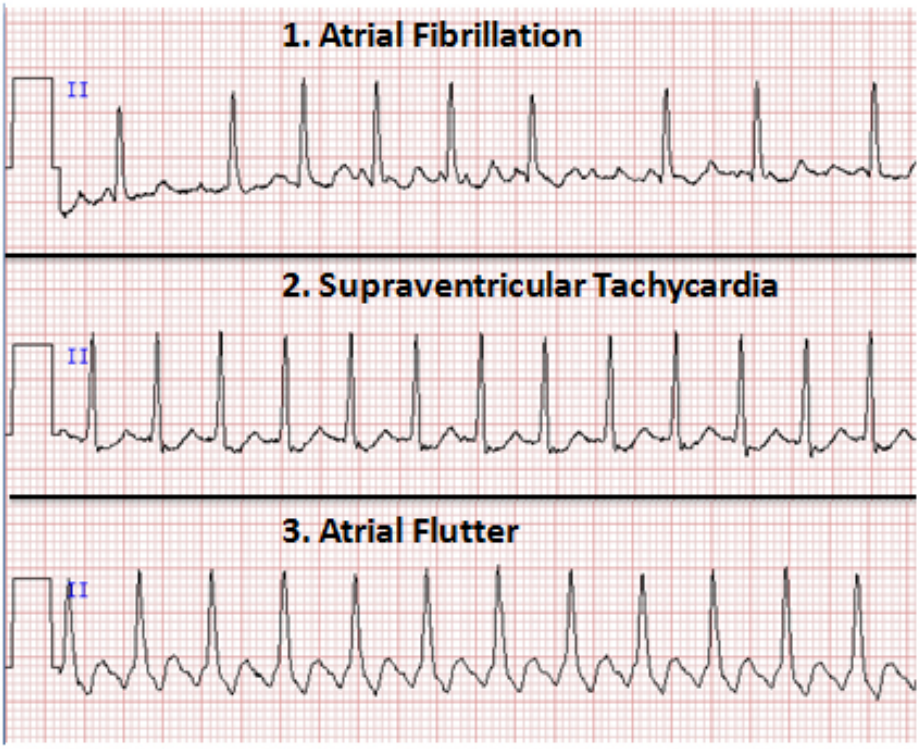

Figure. 1.10: Atrial Fibrillation vs Atrial Flutter vs Tachycardia , taken from [sum17].

Bradycardia

In this type of arrhythmia, the heart beats slower than the normal pace, usually less than 60 beats per minute. This could be because of the disease in electrical heart system.

Tachycardia

In this type of arrhythmia, the heart beats faster than the normal pace, usually, more than 100 beats per minute. when the heart beats too fast, it may not pump blood effectively to the body parts, which could result in shortness of breath.

Heart Block

In this type of arrhythmia, the heart beats slowly because of the delay or complete block of the electrical signal between the upper chambers and the lower chambers of the heart. It is also called atrial ventricular block (AV block).

Bundle Branch Block

Bundle branch block can be of two types, left bundle branch block (LBBB) and right bundle branch block (RBBB). In a normal heart, both bundles depolarized simultaneously and contract at the same time. In this type of arrhythmia, the affected bundle depolarized slowly whereas the un-affected bundle depolarized normally which results in a broader QRS complex, generally longer than 120 milliseconds duration. LBBB and RBBB can be seen in figure 1.11.

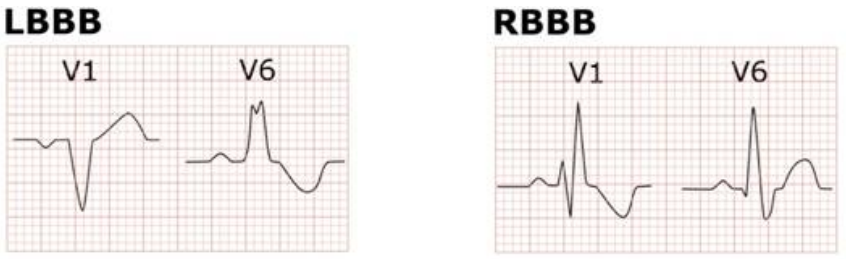

Figure. 1.11: LBBB vs RBBB , taken from [bil17].

2 ECG Signal and Data Processing

2.1 Devices

Wireless sensor devices and contact-less sensor devices are the current trends in the health informatics. The recent improvements in the sensor devices made it possible for the people to bring this idea into reality. When medical sensor devices are combined with cloud computing, it can be thought of as a complete solution for a health care system which not only can be used in hospitals but also can be utilized out of the hospital when the doctor is unreachable regardless of the patients location. Doctors will still be able to monitor his patient condition and according to the patient situation they can instruct the device, that is, attached to the patient, to take appropriate actions. One example can be thought of as a person running somewhere and during that he/she feels some heart pain. Sensors assess the patient's condition and immediately send some notification to the doctor. After looking at the conditions, he sends back a response to the devices, which then acts according to the instruction such as, injects some medicine into the patient body. It can also be used to keep track of the patient location so, in the case of emergency, an ambulance can be instructed to go there. Many of the sensors can be installed in the patient's surrounding, whereas, several sensors can be wearable. These sensors can monitor body temperature, respiration, heart rate, blood pressure, ECG, EEG, etc. Along with sensors, it might be possible that there are several actuators attached to the patient body which is activated by certain events such as, the rise of sugar level in blood.

Multiple contact-less sensor devices are used to implement a system for the thesis, which collect data of the user and process that in real-time. The following devices are used in the implementation:

2.1.1 Magnetic Impedance Sensor

The magnetic impedance (MI) sensor measures the small changes in electrical resistance of the chest or different regions of the body. It uses a special electrodes which emit very low voltage electric current into the body. As the voltage level is very low, therefore, it does not interfere with the heart's electrical system. The MI sensor measures the resistance to the flow of current as it passes through the body via blood, as blood is a good conductor.

During systole, as the blood volume increases, impedance decreases. Similarly, during diastole, the blood volume decreases and the impedance increases.

The MI sensor provides 42 bytes of data packet, which splits into the attributes shown in table 3.1. The byte identifier of the sensor can be seen in the table 3.2.

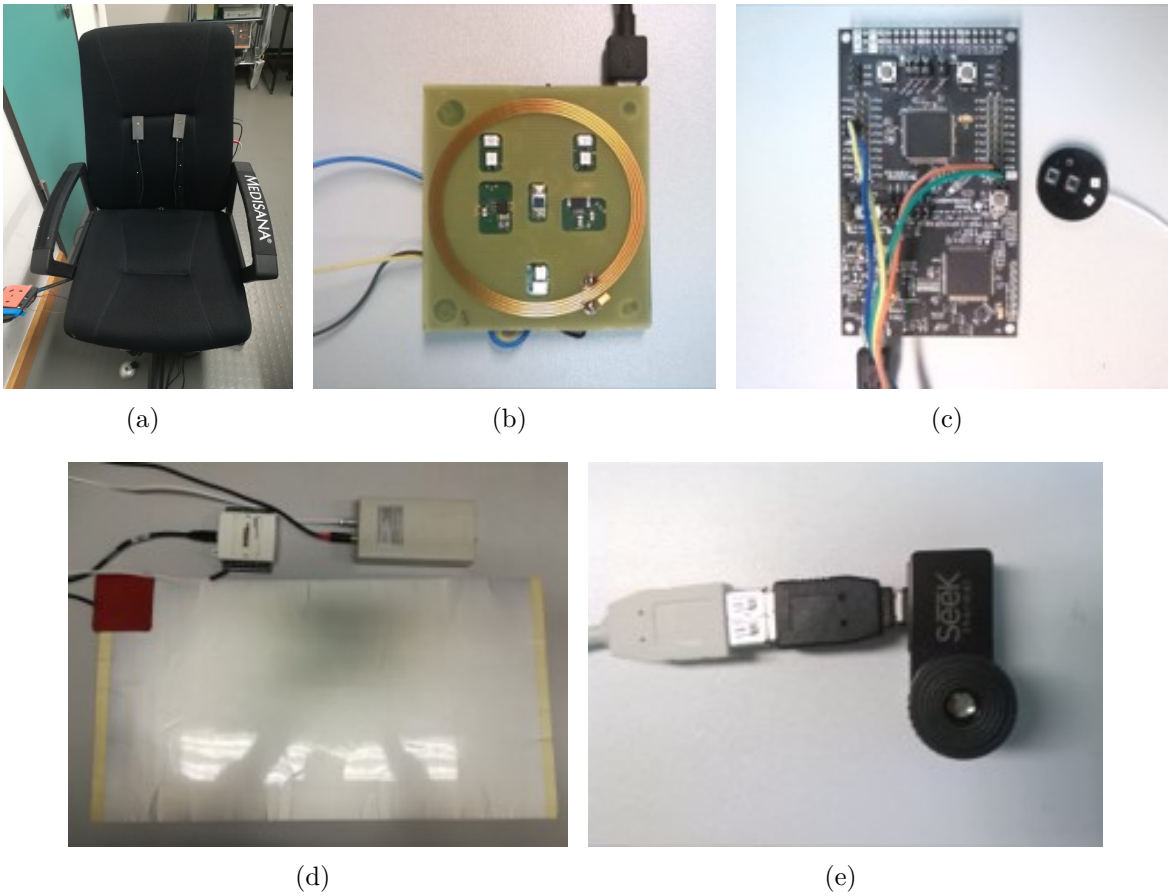

(a) (b) (c)

(d) (e)

Figure. 2.1: A set of sensor devices: (a) an ECG sensor; (b) a MI sensor; (c) a PPG sensor; (d) a BCG sensor; and, (e) a thermal camera.

Tab. 2.1: Attributes of MI s ensor.

Attributes	**Size (Bytes)**
MI_RAW	4
MI	4
RED_RAW	4
ECG_RAW	4
IR_RAW	4
RED_AVG	4
ECG_AVG	4
IR_AVG	4
ACC_X	2
ACC_Z	2
ECG_REF	2
RESP_REF	2
BATTERY	2

There is an exception in the data packet when it contains *0x8101* or *0x8102*. In this case, the size of the data packet may vary according to the no. of count of the corresponding bytes. Moreover, the data packet should be examined and if it contains the corresponding bytes, the data packet should be modified and the bytes *0x8101* should be replaced with *0x81* and *0x8102* should be replaced with *0x82*. This modification has been done in order to differentiate it with the header and data packet identifier as they have the same value.

Tab. 2.2: Byte identifiers for the MI sensor.

2-Byte Identifier	Description
0x81	Header
0x82	Data Packet

2.1.2 Photoplethysmogram Sensor

The Photoplethysmogram (PPG) sensor is used to measures the variations in blood flow in the body which each heart beat. A PPG sensor uses a light source to illuminate the blood and a photo-detector to measures the variations in the light intensity associated with changes in the blood volume. The decrease in light intensity indicates the increase in blood volume and increase in light intensity indicates the decrease in blood volume.

The sensor provides the PPG signal with 4 different channels, a temperature, which is measured in Celsius and accelerometer coordinates. The size of the data changes according to the attributes which can be seen in the table 3.3. The frequency of the data packets changes according to the attributes. The temperature value is sent every one second, whereas, the frequency rate of PPG channels is 100 samples per second. Similarly, for the accelerometer coordinates, the data rate is 50 samples per second.

2.1.3 ECG Sensor

As described in section 1.2, the ECG signal is usually collected by placing electrodes directly on the body but it has several disadvantages as well, which is described in section 1.4. Therefore, non-contact capacitive electrodes has been used to collect the ECG signals of the person. Unlike traditional electrodes, which rely on galvanic contact, the capacitive electrodes are insulated from skin using dielectric material, such as, air gap, clothes, etc. The ECG signal propagates via skin to the dielectric material and then to the electrodes through a capacitive coupling. The major drawback of this approach is that it is very sensitive to body motion.

2.1.4 Ballistocardiogram Sensor

The ballistocardiogram (BCG) sensor measures the ballistic forces associated with cardiac contraction and ejection of blood. These ballistic forces are mainly measures by the electro-

Tab. 2.3: Attributes of PPG Sensor.

2-Byte Identifier	Attributes	Size (Bytes)	Data
0x0050	ppg (8 Bytes)	2	Channel 1
		2	Channel 2
		2	Channel 3
		2	Channel 4
0x0054	Temperature (2 Bytes)	2	Temperature
0x0041	Accelerometer coordinates (6 Bytes)	2	X Coordinate
		2	Y Coordinate
		2	Z Coordinate

mechanical film (EMFi) sensor which converts the mechanical energy into the electrical signal and vice versa. Most of the time, the EMFi sensing device is placed on a chair or bed, which measures the pressure associated with the cardiac activity.

2.1.5 Thermal Camera

A thermal camera is also used to measures the temperature of the person. A thermal seek camera is used for the implementation which captures the thermo temperature images, from which then the temperature is calculated.

2.2 ECG Signal Processing

QRS complex detection is the basis for processing ECG signal. Regardless of what application is required, the accurate detection of QRS complex is a pre-requisite for feature extraction. In order to detect the QRS complex accurately, it is necessary to detect the R-peak position correctly. Once the QRS complex is identified, further examination of the signal can be performed such as heart rate, arrhythmias, classification of ECG signal, ST segment etc. Moreover, P and T waves can be identified correctly.

The "QRS Complexïs the combination of Q, R and S waves and it represents the contraction of the ventricles. It plays a significant role in the detection of cardiac arrhythmias.

Many methods have already been proposed for the detection of QRS complex. These methods fall into 3 categories [PZZ10].

1. Filter Method
2. Artificial Intelligence Method
3. Wavelet transform Method

2.2.1 Filter Method

The filter method use bandpass filter to filter the ECG signal [PT85][RSN97]. In this method, QRS complex is intensify by suppressing the P and T wave. This method is generally very quick and take less time to implement. But the major drawback of this method is that the frequency band of QRS complex and of noise overlapping, affect its performance.

2.2.2 Artificial Intelligence Method

The detection of QRS complex using this method is fast, accurate and more robust. But in reality, it is very time consuming and difficult to implement [XHT92][Pie91][CSCB90]. Therefore, this method is not very popular and not widely used as compared to the other methods.

2.2.3 Wavelet Transform Method

Wavelet transform method becomes very popular in detecting the QRS complex. It is based on time-frequency analysis. It is very efficient and takes less to implement. Many people have already used wavelet transform for detecting the QRS complex. Yazhu Qiu [QDFM06] used Mexican-hat wavelet to detect ECG signal. In the proposed method, although the processing was fast, but it sometimes didn't detect the onset and offset of QRS complex accurately. Nevertheless, it is considered as simple, faster and easier to implement comparatively.

2.3 Wavelet Transform

Transformation is applied to signal in order to get further information about the signal which is not easily available in the raw signal. Most of the time, signals are generally represented in time domain, but in many cases, the important information is hidden in the frequency domain of the signal. Fourier transform is a tool which allows to view the frequency components of the signal. But the major drawback of this transformation is that, a signal can not be viewed in both time and frequency domain at once. Thus, it makes hard to distinguish which frequency components exist at any instance of time. Therefore, a tool was required which helps to view signal in both domain.

Wavelet transform is a very useful tool for analyzing the signal simultaneously in both time and frequency domain [Add17]. It uses a little wavelike functions known as ***wavelets***. Wavelets are used to transform a signal into another representation where signal information can be viewed in a more useful form and this process is known as *wavelet transform*.

Generally there are two operations involved with wavelet. Either they can be stretched or squeezed or can be translated to other locations on the signal and if the wavelet matches the shape of the signal at specific location or scale, it produces a large transform value. And similarly, if the signal and the wavelet do not correlate, it produces a low transformed value. There is a single function called "mother wavelet"which is stretched or translated to produce a family of basis functions known as "daughter wavelets". It is defined as:

$$\Psi_{a,b}(t) = \frac{1}{\sqrt{|a|}}\Psi\left(\frac{t-b}{a}\right), \quad a, b \in \mathbb{R}, a \neq 0 \tag{2.1}$$

where a is the scaling parameter which measures the degree of scale, and b is the translation parameter which measures the time location of the wavelet. If $|a| < 1$, then it mainly corresponds to higher frequencies. And on the other hand, if $|a| > 1$, it corresponds to lower frequencies. It is important to note here that the variation in time and frequency scale of wavelet is supervised by the Heisenberg uncertainty principle. At large scale, the time domain is not very clear, whereas, frequency domain is much finer. As the scale decreases, the frequency domain becomes worse, whereas, time domain becomes finer.

The wavelet transform is defined as:

$$X_W(a,b) = \frac{1}{\sqrt{|a|}}\int_{-\infty}^{\infty} h * \left(\frac{t-b}{a}\right)x(t)\mathrm{d}x \tag{2.2}$$

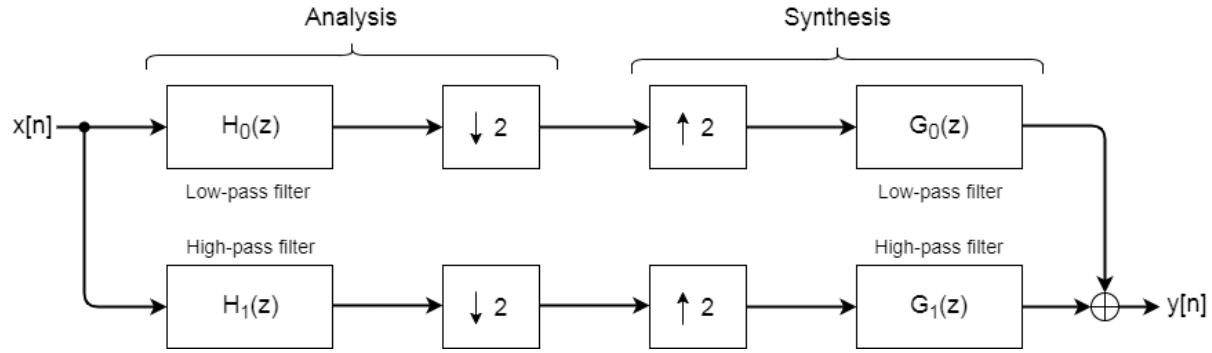

Figure. 2.2: Two-channel filter bank

2.3.1 Continuous Wavelet Transform

2.3.2 Discrete Wavelet Transform

In this thesis, Biorthogonal Spline wavelet is used for detecting the ECG signal. This approach is based on the modulus maxima of zero point to detect the singular point.

For multi-resolution decomposition of signals, a dyadic DWT (discrete wavelet transform) is used where all bandpass filters have different frequency resolution. This is done by first using low-pass and high-pass filters to split the signal into low and high frequency components.

2.4 Biorthogonal Wavelet Transform

2.5 Biorthogonal Spline Wavelet Filter Construction

Let say, $H_0(z)$ and $H_1(z)$ are low-pass filters in the analysis filter bank (decomposition) and $G_0(z)$, $G_1(z)$ are high-pass filters in the synthesis filter bank (reconstruction), as can be seen in the figure 3.2. After passing the input signal $X[n]$ from the filters, the resulting signal is first down-sampled by 2 and then up-sampled by 2 respectively, producing the final output signal $Y[n]$. It is worth to note here that $Y[n]$ is the reconstructed signal.

The idea is to determine H_0, H_1, G_0 and G_1 such that, $Y[n]$ is just a delayed version of input signal $X[n]$. This is called as perfect reconstruction filter bank. A perfect reconstruction filter bank is also known as “biorthogonal“ and the associated filters as biorthogonal filters.

After passing the input signal from the channel 1, it will produce:

$$Y_0(z) = \frac{1}{2}G_0(z)[H_0(z)X(z) + H_0(-z)X(-z)] \tag{2.3}$$

Similarly, for the 2nd channel, it will produce:

$$Y_1(z) = \frac{1}{2}G_1(z)[H_1(z)X(z) + H_1(-z)X(-z)] \tag{2.4}$$

Adding the output of these 2 channels will produce the final output.

$$\begin{aligned} Y(z) &= Y_0(z) + Y_1(z) \\ &= \frac{1}{2}G_0(z)[H_0(z)X(z) + H_0(-z)X(-z)] + \frac{1}{2}G_1(z)[H_1(z)X(z) + H_1(-z)X(-z)] \end{aligned} \tag{2.5}$$

Arranging $Y(z)$ in such a way so that, one part should depends on $X(z)$ and the other part on $X(-z)$. We get,

$$Y(z) = \frac{1}{2}[G_0(z)H_0(z) + G_1(z)H_1(z)]X(z) + \frac{1}{2}[G_0(z)H_0(-z) + G_1(z)H_1(-z)]X(-z) \tag{2.6}$$

The important thing to note here is that, $X(-z)$ is the aliasing part, and $X(z)$ is the distortion part.

2.5.1 Design of Biorthogonal Spline Wavelet Filter

The perfect reconstruction for filter bank can be achieved if the following two conditions are satisfied.

1. No aliasing:
$$G_0(z)H_0(-z) + G_1(z)H_1(-z)]X(-z) = 0 \tag{2.7}$$

2. No distortion:
$$G_0(z)H_0(z) + G_1(z)H_1(z) = mz^{-k} \tag{2.8}$$

where m is constant and k is a time delay.

In order to satisfy condition 1 i.e., to get rid of aliasing, one can do:

$$\begin{aligned} G_0(z) &= H_1(-z), \\ G_1(z) &= -H_0(-z) \end{aligned} \tag{2.9}$$

So now, we only need to find two filters values instead of four. Lets assume that,

$$P_0(z) = G_0(z)H_0(z) \tag{2.10}$$

From equation 3.9 and 3.10, we can deduce:

$$G_1(z)H_1(z) = -H_0(-z)G_0(-z) = -P_0(-z) \tag{2.11}$$

After getting these values, the condition 2 (no distortion) can be re-written as:

$$P_0(z) - P_0(-z) = mz^{-k} \tag{2.12}$$

In the above equation, only one filter value is required i.e., $P_0(z)$ (also called half band filter). The perfect reconstruction conditions naturally implies that the both analysis and the synthesis filters are biorthogonal to each other, i.e., a biorthogonal filter bank makes sure that synthesis filter bank is the inverse of analysis filter bank.

2.5.2 Steps for Designing FIR Filter Bank

The steps for designing FIR filter bank can be summarized as:

1. Design a low-pass filter for $P_0(z)$ which satisfy the equation 3.13. One option is to use Daubechies function to find the value for $P_0(z)$:

$$P_0(z) = (1 + z^{-1})^{2p} Q(z) \tag{2.13}$$

   where p can be any integer and $Q(z)$ be a polynomial of degree $(2p - 2)$.

2. Factorize $P_0(z)$ to get the values for $G_0(z)$ and $H_0(z)$.

3. Find the filter coefficients for high-pass filters using the equations 3.9.

Lets assume that, $P = 2$ and and $Q(z)$ be a quadratic polynomial $(a + bz^{-1} + cz^{-2})$. Substituting these values in equation 3.13 will produce a polynomial of degree z:

$$P_0(z) = (1 + z^{-1})^4(a + bz^{-1} + cz^{-2}) \tag{2.14}$$

Substituting $a = c = -\frac{1}{16}, b = 4$, we get:

$$P_0(z) = \frac{(1 + z^{-1})^4(-1 + 4z^{-1} + z^{-2})}{16} \tag{2.15}$$

Factorizing $P_0(z)$ to get $H_0(z)$ and $G_0(z)$. Lets say we get:

$$\begin{aligned} H_0(z) &= \frac{(1 + z^{-1})^3}{4} \\ &= \frac{(1 + 3z^{-1} + 3z^{-2} + z^{-3})}{4} \end{aligned} \tag{2.16}$$

and

$$\begin{aligned} G_0(z) &= \frac{(1 + z^{-1})(-1 + 4z^{-1} + z^{-2})}{4} \\ &= \frac{(-1 + 3z^{-1} + 3z^{-2} - z^{-3})}{4} \end{aligned} \tag{2.17}$$

Then by equation 3.13, we have:

$$\begin{aligned} H_1(z) = G_0(-z) \\ = \frac{(-1 - 3z^{-1} + 3z^{-2} + z^{-3})}{4} \end{aligned} \tag{2.18}$$

and

$$G_1(z) = -H_0(-z) \\ = \frac{(-1 + 3z_3^{-1}z^{-2} + z^{-3})}{4} \tag{2.19}$$

Therefore, the filter coefficients are:

$$\begin{aligned} h_0(0) &= \frac{1}{4} & h_0(1) &= \frac{3}{4} \\ h_0(2) &= \frac{3}{4} & h_0(3) &= \frac{1}{4} \\ h_1(0) &= \frac{-1}{4} & h_1(1) &= \frac{-3}{4} \\ h_1(2) &= \frac{3}{4} & h_1(3) &= \frac{1}{4} \\ g_0(0) &= \frac{-1}{4} & g_0(1) &= \frac{3}{4} \\ g_0(2) &= \frac{3}{4} & g_0(3) &= \frac{-1}{4} \\ g_1(0) &= \frac{-1}{4} & g_1(1) &= \frac{3}{4} \\ g_1(2) &= \frac{-3}{4} & g_1(3) &= \frac{1}{4} \end{aligned} \tag{2.20}$$

2.6 Mallat's Algorithm

The binary wavelet transform or dyadic wavelet transform of a signal $f(n)$ can be calculated by using Mallat algorithm [MH92] as follows:

$$s_{2^j} f(n) = \sum h_k s_{2^{j-1}} f(n - 2^{j-1}k), \tag{2.21}$$

$$w_{2^j} f(n) = \sum g_k s_{2^{j-1}} f(n - 2^{j-1}k). \tag{2.22}$$

where, $s_{2^0} f(n)$ is the original signal to be processed. In our case, it is ECG signal. $w_{2^j} f(n)$ is the wavelet coefficient i.e., the dyadic wavelet transform of the signal and $s_{2^j} f(n)$ is the approximation coefficient for the scale j. h_k and g_k are the coefficients of low-pass filter and high-pass filter respectively which are defined in the equation 3.20. The signal is

decomposed into several frequency bands at certain scale j and then the frequency bands which have noises, are set to zero. And by using the synthesis filters, the de-noised signal can be reconstructed.

2.7 Using Wavelet Transform to Identify Singular Point of QRS Complex

2.7.1 Feature Extraction Using Wavelets

Most of the time, the important information of signal resides on the irregularities and singularities of the signal and wavelets can be used to extract those information. When the filter bank and wavelets are chosen appropriately, the wavelets are able to capture the irregularities and singularities of the signal. Mathematically, the local singularity of a signal is measured using Lipschitz exponent, the inflection points of signal $f(n)$ appear as extrema at $\frac{df(t)}{dt}$ and as zero crossing points at $\frac{d^2f(t)}{dt}$. Therefore, Mallat has suggested to use a wavelets which is the first derivative of a scaling function.

2.7.2 Lipschitz Exponent

The functions which are infinitely differentiable are described as smooth or with no singularity [XCWX13]. If at some point, the function has non continuous derivative, then the point is known as singular point. The Lipschitz exponent is a good application to measure the singularity of the point.

2.7.3 Relationship between Lipschitz Exponent and Modulus Maximum

Mallat has shown in his paper [MH92] that, all signals and noise in their may be completely represented by their singularities and singularities are generally referred in terms of Lipschitz exponents. If a signal is n times differentiable at time t_0, then its nth derivative is singular and it will be described as Lipschitz α where $\alpha > n$. If a signal is continuously differentiable at time t_0, then it is non-singular and has Lipschitz exponent 1.

Signals can have negative Lipschitz exponent as well. For example, many signals have singularities with positive Lipschitz exponents whereas, noise has negative Lipschitz exponent. Therefore, having this mind, it makes it possible to separate a signal from noise if the singularities of noise can be detected and separated.

Tab. 2.4: Wavelet Transform ECG Signal Frequency Range

Transform Scale	Frequency Range (Hz)
2^1	90.0~180.0
2^2	29.92~84.24
2^3	1.52~38.88
2^4	5.76~19.44

Generally, it is known that the singularity of a signal is directly proportional to the Lipschitz exponent. Therefore, as the transform scale increases, the wavelet transform modulus maxima will also get increases (Lipschitz exponent > 0) and similarly it will decreases when Lipschitz exponent < 0. It can be seen that R wave in the original ECG signal appears as a pair of positive and negative extreme in the waveform which resulted after the decomposition of wavelet transform.

2.8 Dataset

The MIT-BIH Arrhythmia dataset is used for the implementation of the system. It contains 48 hours of recording of 47 subjects. Each record contains 2 signals, namely MLII and V5, with a recording of 30 minutes duration. The sample rate for the recording is 360 samples per second per channel with 11 bit resolution over a 10mV range. Each record consists of 3 files:

- Header file (.hea): It contains information such as number of samples, sampling frequency, ECG signal format, number of ECG leads and their types, patient‘s history and the detailed clinical information.
- ECG signals (.dat): It contains the original signal values of both MLII and V5 leads. The signals from MLII lead are considered only for the analysis.
- Attribute file (.atr): It contains the annotation information of the ECG signal, annotated by the doctors.

There is a specific python package available, wfdb-python for reading the data from the MIT-BIH dataset. The ECG signals of one of the patients can be seen in Figure 3.3. It contains 2 signals, namely, MLII and V5.

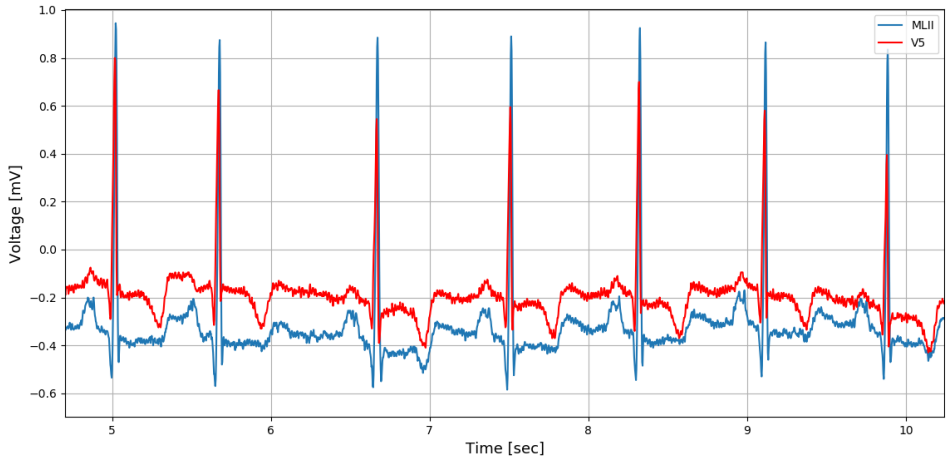

Figure. 2.3: The ECG signals from MIT-BIH dataset.

The signals are in a raw form and need to be processed before they can be used. Most of the time, the signals are also contaminated with noise, baseline drift, etc. and they are required to be cleaned to get the correct values.

2.9 Preprocessing

The ECG signal is required to be processes before it is analyzed, as it contains several noises and artifacts. The most common noises are the baseline wander and 60Hz power interference. Baseline wander generally appears because of the subject respiration or the body movements. It has a frequency range of 0Hz to 0.5Hz. The power interference affects the signals because of the electrical appliances in the surrounding.

Two different methods has been used to remove the noise and artifacts from the signal in the system implementation.

1. Wavelet Transform Method

2. Band-pass Filter Method

2.9.1 Wavelet Transform Method

The wavelet transform is a very interesting technique for analyzing the signal in the time-frequency domain. It distributes the signal in such a way that the resulting block is well

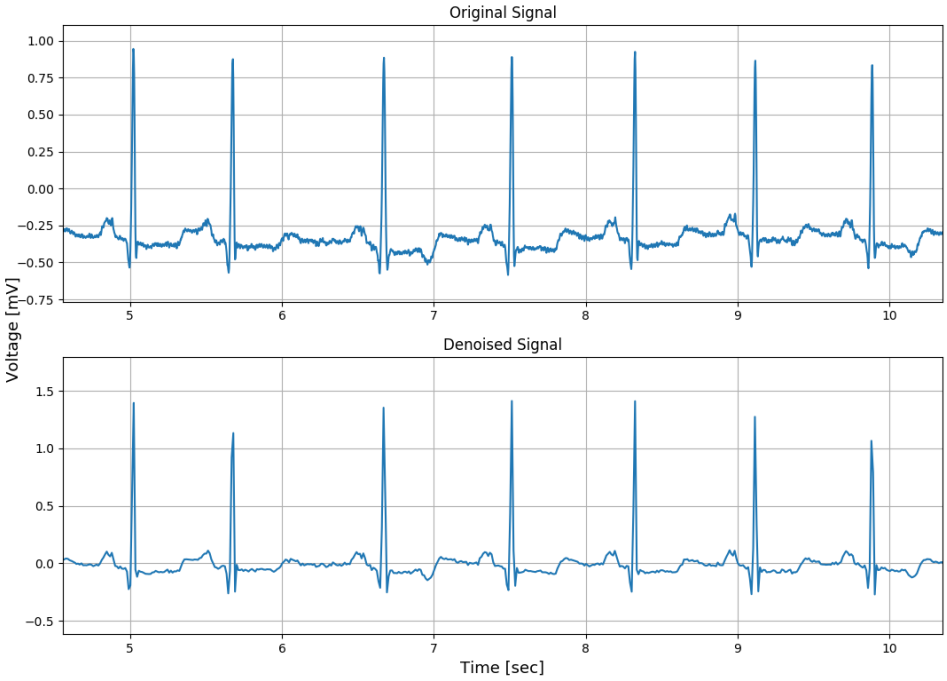

Figure. 2.4: The filtered ECG signal using wavelet.

localized in both time and frequency. Decomposition of the signal into different frequency bands is obtained by passing the signal through high-pass and low-pass filter respectively, which results in 2 sets of coefficients namely, approximation coefficients and detail coefficients. The approximation coefficients contain the low-pass filter output and the detail coefficients contain the high-pass filter output. The next step split the approximation coefficients again into 2 parts using the same process and so on.

The original signal contains the high-frequency noise and the baseline drift. The wavelet transform can be used to remove the corresponding noises and the baseline drift. The process starts by decomposing the original signal into 8 layers using wavelet type bior2.6, which results in the corresponding detail and approximation coefficients. Mostly, the layers 1 and 2 of the detail coefficients contain the high-frequency noise and the layer 8 of the approximation coefficients contain the baseline drift. Therefore, the layers 1 and 2 of the detail coefficients and layer 8 of the approximation coefficients are set to 0; which then results in the de-noised signal with no baseline drift. The resulting ECG signal can be seen in the Figure 3.4.

2.9.2 Band-pass Filter Method

A band-pass filter is a type of filter which passes only frequencies in a certain range or spread without disturbing the input signal. The range of frequencies, let say, f1 and f2, are called the frequency passband.

Band-pass filter can be used to reduce the baseline drift, motion artifacts and high-frequency noise from the ECG signal. A passband of 3 Hz to 45 Hz has been used. After passing the ECG signal through the band-pass filter, the resulting signal produced is the de-noised signal with no high-frequency and baseline drift. The de-noised signal can be seen in the Figure 3.5.

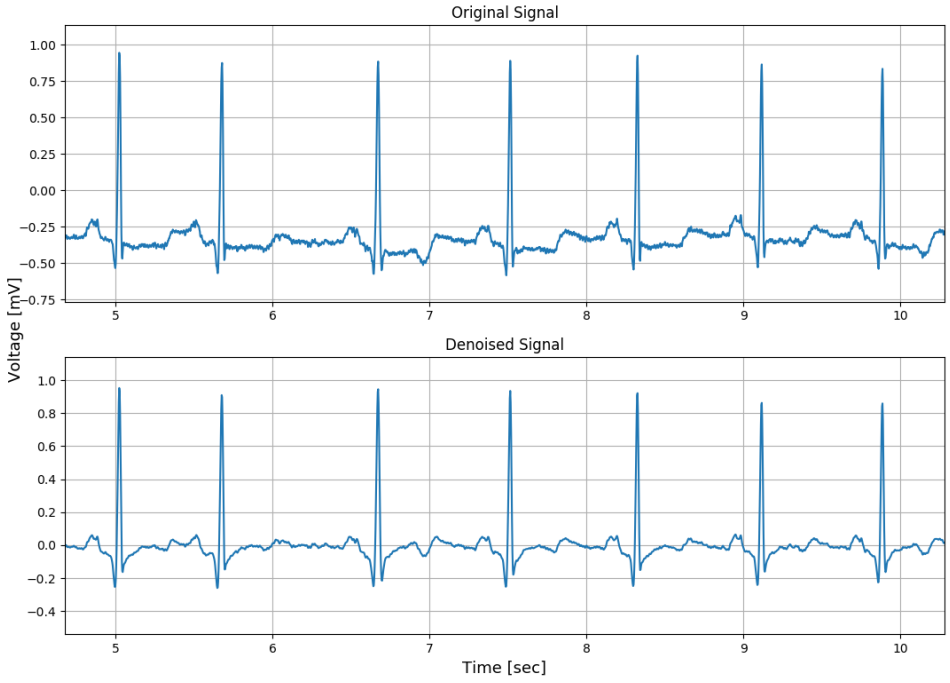

Figure. 2.5: The filtered ECG signal using bandpass filter.

2.10 QRS Detection

QRS detection is the basis for processing ECG signal. Regardless of what application is required, the accurate detection of QRS is a pre-requisite for feature extraction. A good wavelet base can help detect the features of ECG signal more appropriately with speed and accuracy. Therefore, Biorthogonal spline wavelet is used to detect QRS wave. Biorthogonal

spline wavelet transform of ECG signal is calculated using the Mallat algorithm. Figure 3.6 shows the Biorthogonal spline wavelet transform of ECG signal at 4 different scales.

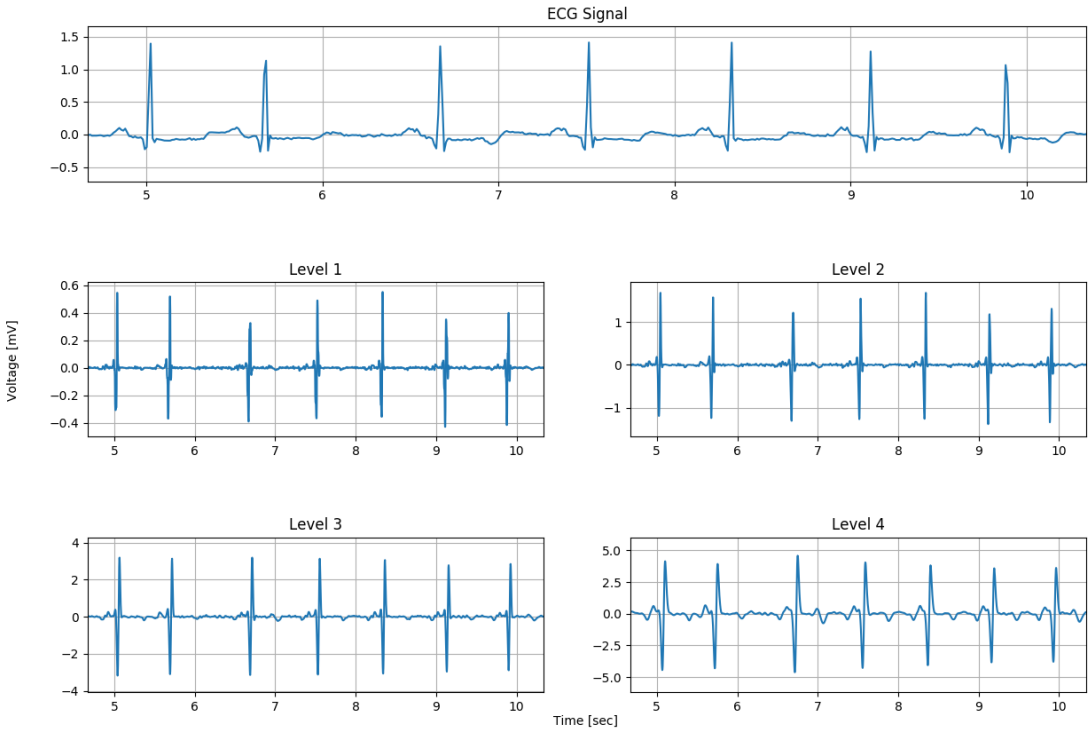

Figure. 2.6: ECG signal and its decomposition at different scales.

Most of the QRS complex energy lies in the 3rd scale, therefore, we can use the maximal minimal method in the 3rd layer of the detail coefficient to find the R waves. The process starts by taking the first derivative of the 3rd layer to find the maximum and minimum points and then the 2nd derivative to locate the actual maximum and minimum values. The resulting waves are shown in Figure 3.7. As it can be seen that, there are other peaks available as well, therefore, to get the maximum and minimum pair only, a threshold needs to be set. And all the values that do not fulfill the threshold should be discarded. For finding the threshold, the result of the 2nd derivative is divided into 4 parts and from each part, the maximum value is located. After getting the values, the average is calculated for these values and that average is then divided by 3. The resultant value is a new threshold. The pair can be seen in Figure 3.8.

The value of R wave lies at the zero-crossing point (with a little delay) which is between the maximum and the minimum value pair. For compensating the delay, a maximum value can be searched in the window of 20 points to the zero-crossing point. The detected R-peaks can be seen in Figure 3.9.

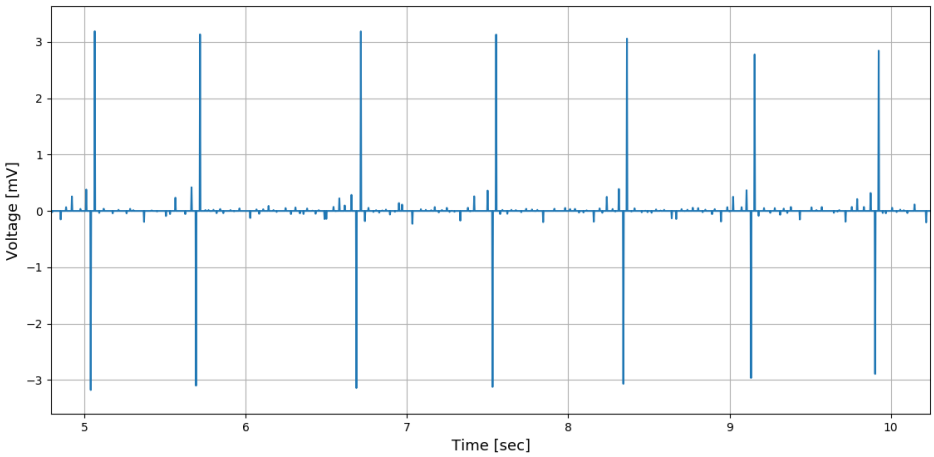

Figure. 2.7: Maximum and minimum values on scale 3.

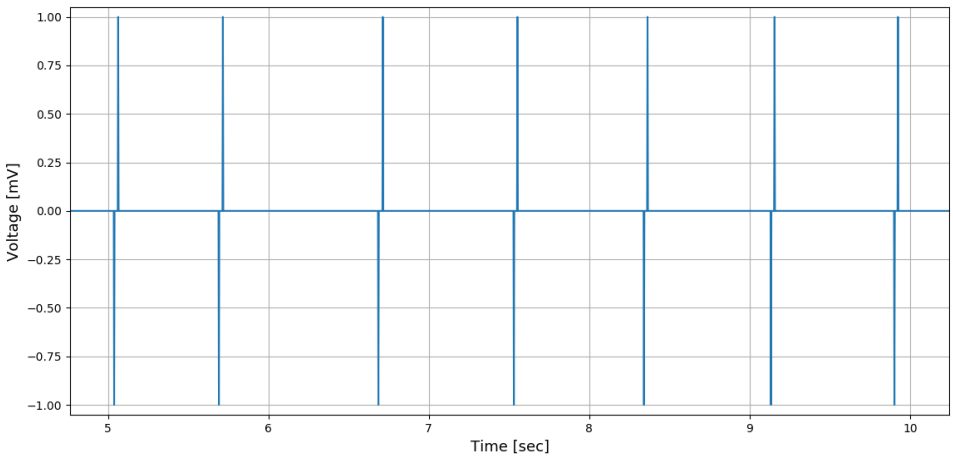

Figure. 2.8: Maximum and minimum values pair for finding the R peaks.

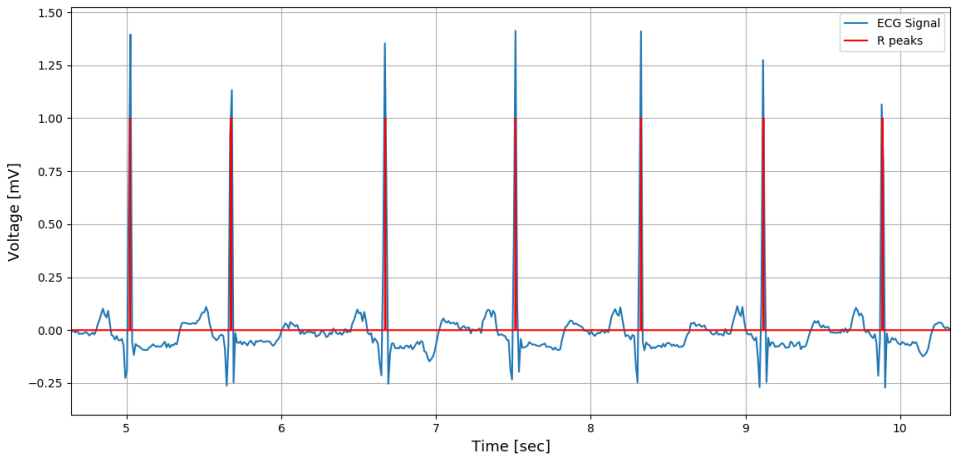

Figure. 2.9: Detected R peaks.

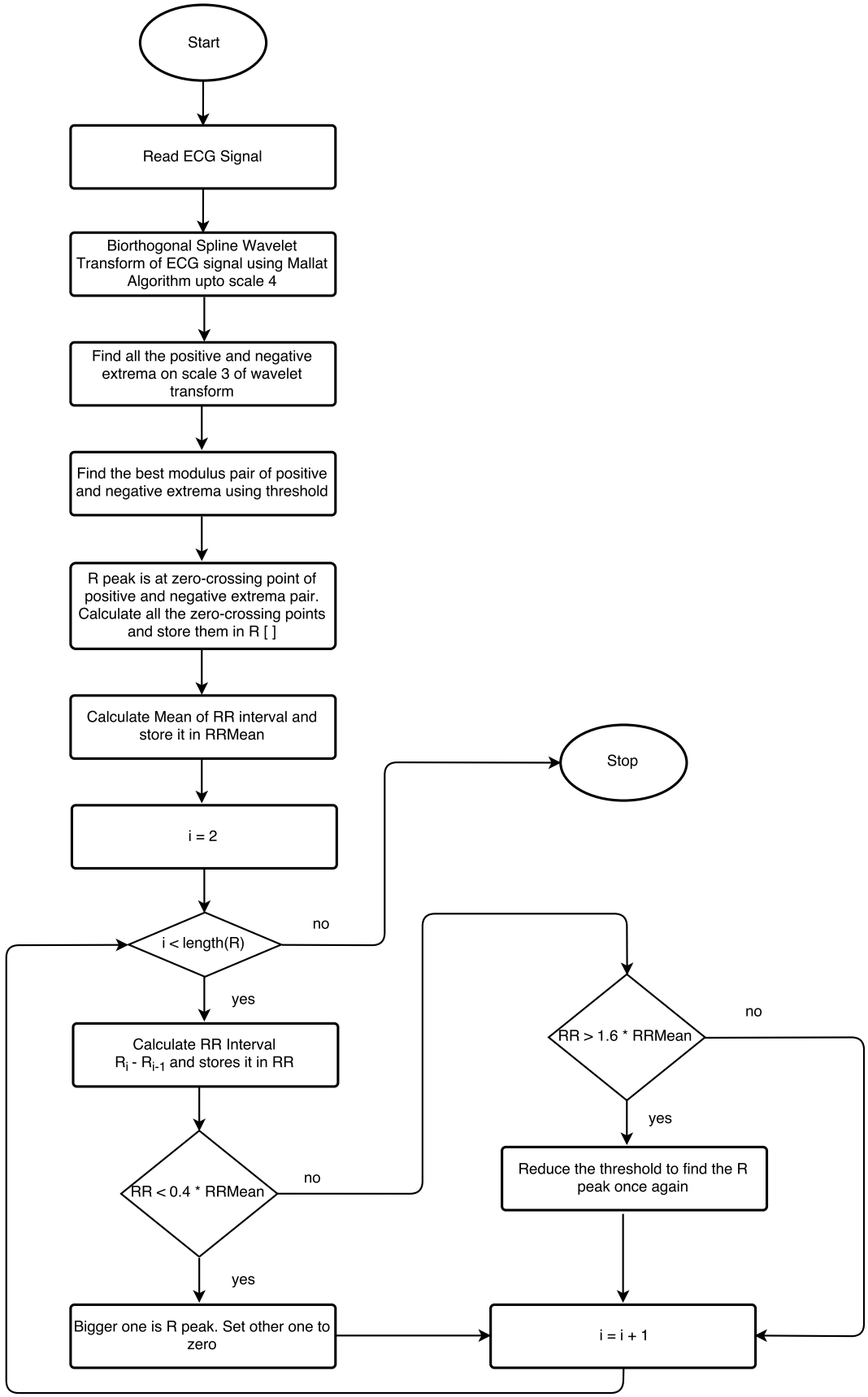

Figure. 2.10: R peak flow chart.

Literaturverzeichnis

[Add17] Addison, P.S.: *The Illustrated Wavelet Transform Handbook: Introductory Theory and Applications in Science, Engineering, Medicine and Finance, Second Edition*. CRC Press, 2017 https://books.google.de/books?id=wBoNDgAAQBAJ. – ISBN 9781482251333

[bil17] bilagi: *arrhythmia*. http://bilagi.org/blog/2016/08/24/chapter-9-ventricular-conduction-abnormalities/. Version: 2017. – [Online; accessed 13-December-2017]

[Com17a] Commons, Wikimedia: *File:Brantigan 1963 1-53.png — Wikimedia Commons, the free media repository*. https://commons.wikimedia.org/w/index.php?title=File:Brantigan_1963_1-53.png&oldid=229447194. Version: 2017. – [Online; accessed 8-November-2017]

[Com17b] Commons, Wikimedia: *File:Limb leads.svg — Wikimedia Commons, the free media repository*. https://commons.wikimedia.org/w/index.php?title=File:Limb_leads.svg&oldid=262129086. Version: 2017. – [Online; accessed 8-November-2017]

[Com17c] Commons, Wikimedia: *File:SinusRhythmLabels.svg — Wikimedia Commons, the free media repository*. https://commons.wikimedia.org/w/index.php?title=File:SinusRhythmLabels.svg&oldid=260036882. Version: 2017. – [Online; accessed 8-November-2017]

[con17] contributors, Wikipedia: *Premature ventricular contraction — Wikipedia, The Free Encyclopedia*. https://en.wikipedia.org/w/index.php?title=Premature_ventricular_contraction&oldid=810563186. Version: 2017. – [Online; accessed 23-December-2017]

[CSCB90] Coast, D. A. ; Stern, R. M. ; Cano, G. G. ; Briller, S. A.: An approach to cardiac arrhythmia analysis using hidden Markov models. In: *IEEE Transactions on Biomedical Engineering* 37 (1990), Sept, Nr. 9, S. 826–836. http://dx.doi.org/10.1109/10.58593. – DOI 10.1109/10.58593. – ISSN 0018–9294

[LD] Limaye, Mr H. ; Deshmukh, Mrs V.: ECG Noise Sources and Various Noise Removal Techniques: A Survey.

[mau17] mauvila: *ECG artifcats*. http://www.mauvila.com/ECG/ecg_artifact.htm. Version: 2017. – [Online; accessed 12-November-2017]

[med17] MEDICINENET: *arrhythmia*. https://www.medicinenet.com/arrhythmia_irregular_heartbeat/article.htm. Version: 2017. – [Online; accessed 13-December-2017]

[MG13] MARKOVSKI, S. ; GUSEV, M.: *ICT Innovations 2012: Secure and Intelligent Systems*. Springer Berlin Heidelberg, 2013 (Advances in Intelligent Systems and Computing). https://books.google.de/books?id=mWtHAAAAQBAJ. – ISBN 9783642371691

[MH92] MALLAT, S. ; HWANG, W. L.: Singularity detection and processing with wavelets. In: *IEEE Transactions on Information Theory* 38 (1992), March, Nr. 2, S. 617–643. http://dx.doi.org/10.1109/18.119727. – DOI 10.1109/18.119727. – ISSN 0018–9448

[MPS+11] MITHUN, P. ; PANDEY, P. C. ; SEBASTIAN, T. ; MISHRA, P. ; PANDEY, V. K.: A wavelet based technique for suppression of EMG noise and motion artifact in ambulatory ECG. In: *2011 Annual International Conference of the IEEE Engineering in Medicine and Biology Society*, 2011. – ISSN 1094–687X, S. 7087–7090

[Pie91] PIETKA, Ewa: Feature extraction in computerized approach to the ecg analysis. In: *Pattern Recognition* 24 (1991), Nr. 2, 139 - 146. http://dx.doi.org/https://doi.org/10.1016/0031-3203(91)90083-H. – DOI https://doi.org/10.1016/0031–3203(91)90083–H. – ISSN 0031–3203

[PT85] PAN, J. ; TOMPKINS, W. J.: A Real-Time QRS Detection Algorithm. In: *IEEE Transactions on Biomedical Engineering* BME-32 (1985), March, Nr. 3, S. 230–236. http://dx.doi.org/10.1109/TBME.1985.325532. – DOI 10.1109/TBME.1985.325532. – ISSN 0018–9294

[PZZ10] PAN, T. ; ZHANG, L. ; ZHOU, S.: Detection of ECG characteristic points using Biorthogonal Spline Wavelet. In: *2010 3rd International Conference on Biomedical Engineering and Informatics* Bd. 2, 2010. – ISSN 1948–2914, S. 858–863

[QDFM06] QIU, Yazhu ; DING, Xianfeng ; FENG, Jun ; MO, Zhiwen: [QRS complexes detection based on Mexican-hat wavelet]. In: *Sheng wu yi xue gong cheng xue za zhi = Journal of biomedical engineering = Shengwu yixue gongchengxue zazhi* 23 (2006), December, Nr. 6, 1347?1349. http://europepmc.org/abstract/MED/17228741. – ISSN 1001–5515

[RSN97] RUHA, A. ; SALLINEN, S. ; NISSILA, S.: A real-time microprocessor QRS detector system with a 1-ms timing accuracy for the measurement of ambulatory HRV. In: *IEEE Transactions on Biomedical Engineering* 44 (1997),

March, Nr. 3, S. 159–167. http://dx.doi.org/10.1109/10.554762. – DOI 10.1109/10.554762. – ISSN 0018–9294

[Sch17] SCHOOLINFO: *Electrical activity of Heart*. http://schoolbag.info/biology/mcat/32.html. Version: 2017. – [Online; accessed 12-November-2017]

[sum17] SUMDU: *arrhythmia*. https://elearning.sumdu.edu.ua/free_content/lectured:a3664646bdd2fb5e12ac4d9fc4d3dff83793be56/20150113065426//64025/index.html. Version: 2017. – [Online; accessed 13-December-2017]

[The] THE UNIVERSITY OF NOTTINGHAM: *Chest Leads*. – [Online; accessed 8-November-2017]

[XCWX13] XING, S. ; CHEN, S. ; WEI, Z. ; XIA, J.: *Unifying Electrical Engineering and Electronics Engineering: Proceedings of the 2012 International Conference on Electrical and Electronics Engineering*. Springer New York, 2013 (Lecture Notes in Electrical Engineering). https://books.google.de/books?id=plq4BAAAQBAJ. – ISBN 9781461449812

[XHT92] XUE, Q. ; HU, Y. H. ; TOMPKINS, W. J.: Neural-network-based adaptive matched filtering for QRS detection. In: *IEEE Transactions on Biomedical Engineering* 39 (1992), April, Nr. 4, S. 317–329. http://dx.doi.org/10.1109/10.126604. – DOI 10.1109/10.126604. – ISSN 0018–9294